

# Multi-Link Level Simulation Model of Indoor Peer-to-Peer Radio Channels

Paolo Castiglione\*, Claude Oestges<sup>†</sup>, Nicolai Czink\*, Bernd Bandemer<sup>‡</sup>,  
Florian Kaltenberger<sup>§</sup> and Arogyaswami Paulraj<sup>‡</sup>

\*FTW Forschungszentrum Telekommunikation Wien, Vienna, Austria  
{czink, castiglione}@ftw.at

<sup>†</sup>ICTEAM Electrical Engineering, Université catholique de Louvain, Louvain-la-Neuve, Belgium  
claude.oestges@uclouvain.be

<sup>‡</sup>Smart Antennas Research Group, Stanford University, Stanford, CA, USA  
{bandemer, apaulraj}@stanford.edu

<sup>§</sup>Mobile Communications Department, Eurecom, Sophia-Antipolis, France  
florian.kaltenberger@eurecom.fr

**Abstract**—This paper presents a link-simulation model for cooperative indoor communication systems at 2.4 GHz, based on empirical data. The channel simulator relies on a simple formulation, and takes into account the impact of the node mobility on fading and shadowing statistics. This implementation is then applied to the evaluation of the cooperative system performance in terms of network lifetime.

## I. INTRODUCTION

In peer-to-peer networks, cooperation is a promising technology to increase reliability and spectral efficiency [1], [2]. The basic idea is to allow nodes to “help” other nodes with their communication by exploiting the broadcast nature of the wireless channel. In such networks, especially when the distributed multi-link channel is non-homogeneous, the selection of the best relay can even provide better performance compared to existing distributed space-time codes [3]. A particularity of cooperative systems is that shadowing correlation between different links can significantly affect the performance of the network compared to the case where the shadow fading is assumed to be identically and independently distributed (i.i.d.) [4], [5]. Additionally, the peer-to-peer channel statistics, including the aforementioned shadowing correlation, might be significantly affected by the node mobility. As some nodes might move, while other nodes might remain static, we make a distinction between three types of mobility:

- *single-mobile* scenarios: either the receiver (Rx) or transmitter (Tx) is moving,
- *double-mobile* scenarios: terminals at both link ends are moving,
- *nomadic* scenarios: both terminals are static, although they can be located almost anywhere in the region of interest, most often in non line-of-sight from each other.

The goal of this paper is to propose a multi-link simulation model for peer-to-peer cooperative (a.k.a. distributed) radio channels based on the experimental results of [6], [7]. We first summarize the main results of [6], [7], and then propose

a model implementation under the form of a generic model whose parameters are extracted from measured data. A typical application is then outlined illustrating how the channel impacts the partner selection in indoor cooperative networks.

## II. EXPERIMENTAL RESULTS

In [6], [7], indoor-to-indoor (I2I) distributed channels were analyzed based on a wideband experimental campaign at 2.4 GHz. The main findings can be summarized as follows:

- To accurately account for the different node mobility scenarios in distributed channels, shadowing was divided into static and dynamic shadowing, the former being time-invariant and defined as the difference between the average received power at a given location to the received power predicted by a deterministic path-loss law.
- For nomadic links, the standard deviation of lognormal dynamic shadowing is positively correlated with the range. For mobile links, it is similar at all ranges.
- In all cases, the dynamic shadowing correlation can be high (positively or negatively) and is related to the node mobility: the average correlation between two links is found to be more positive when both links share a common moving node.
- For nomadic scenarios, small-scale fading is well approximated by a Ricean or a m-Nakagami distribution whose parameters (K-factor and m-parameter) decrease with increasing range.
- For mobile transmissions, the fading amplitude can be modeled by a single distribution consisting of a weighted combination of Ricean and Double-Rayleigh distributions. The Double-Rayleigh fading component is significantly stronger when both Tx and Rx nodes are moving as opposed to only one of them moving.

In addition to the results detailed above, a further and finer analysis reveals that in nomadic channels, static shadowing

itself can be divided into two contributions: (i) a frequency-invariant (or space-invariant) obstruction loss, which is common with mobile links, and (ii) a spatial fading related term, which models the static multipath interference. In that sense, this part of static shadowing, which only exists for static links, has the same origin as spatial, or equivalently, frequency-selective fading. Since this contribution does not lead to any temporal variation, we have decided to include it under the shadowing contribution, rather than into fading. This is a particularity of nomadic links, where temporal and spatial (or frequency) fading behaviors are unrelated as they are caused by different mechanisms. Therefore, they must be modeled on a separate basis, by contrast to mobile scenarios, where static shadowing only represents the classical time-invariant obstruction of the link (e.g. by fixed furniture or static people), and is thus frequency/space invariant.

### III. MODEL IMPLEMENTATION

The narrowband complex channel  $h_{mn}$  from indoor node  $m$  to indoor node  $n$  is described by

$$h_{mn}(t) = \frac{1}{10^{L_{mn}/20} \cdot 10^{\tilde{S}_{mn}(t)/20}} \cdot g_{mn}(t). \quad (1)$$

The various contributions are modeled as described in the following sections.

#### A. Path Loss and Static Shadowing

The path loss and static shadowing combined in  $L_{mn}$  are modeled as outlined by

$$L = L_0 + 1.75 \cdot 10 \log_{10} \left( \frac{d}{d_0} \right) + \bar{S}_o - 20 \log_{10} \bar{s}_s, \quad (2)$$

where  $d = d_{mn}$  is the range, and  $L_0$  is the reference path-loss in line-of-sight at  $d_0 = 1$  m. We further consider that the obstruction loss  $\bar{S}_o$  is a zero-mean Gaussian variable of standard deviation  $\sigma_{\bar{S}_o}$  equal to 4.4 (for fixed nodes) and 4.6 (for mobile nodes), that  $\bar{s}_s$  is Rayleigh distributed for static nodes, whereas  $\bar{s}_s = 1$  for mobile scenarios.

#### B. Dynamic Shadowing

The parameter  $\tilde{S}_{mn}(t)$  is a time-varying zero-mean Gaussian variable, whose standard deviation  $\sigma_{\tilde{S}}$  is modeled differently for nomadic and mobile links, as shown below. The shadowing temporal auto-correlation is modeled as a decreasing exponential, whose decay time  $\tau = 2.5$  s for static links, and given by  $d_c v^{-1}$  for mobile links, with  $d_c = 0.45$  m and  $v$  being the node speed (indeed,  $d_c$  is the variable independent from the terminal's speed in mobile scenarios). The shadowing correlation coefficient  $C[m, n, m', n']$  between links  $(n, m)$  and  $(n', m')$  is a function of the mobility scenario and the number of joint moving nodes, as explained in [6]. It is generated by a truncated Gaussian distribution  $\mathcal{N}_{[-1,1]}(\mu_C, \sigma_C)$ , whose parameters are given in Table I. Hence, to model the dynamic shadowing  $\tilde{S}_{mn}(t)$  and  $\tilde{S}_{m'n'}(t)$  on two links over  $T$  time samples ( $t = [1, \dots, T]$ ),

- Use the following auto-regressive process to generate autocorrelated dynamic shadowing values,

$$x(t) = e^{-1/\tau} x(t-1) + \sqrt{1 - e^{-2/\tau}} g_x(t), \quad (3)$$

$$y(t) = e^{-1/\tau} y(t-1) + \sqrt{1 - e^{-2/\tau}} g_y(t), \quad (4)$$

where  $g_x$  and  $g_y$  are both time series of length  $T$ , whose values are drawn independently from a normal distribution  $\mathcal{N}(0, 1)$ . This ensures an autocorrelation  $E\{x(t)x(t+\Delta t)\} = e^{-|\Delta t|/\tau}$ , and similar for  $y(t)$ .

- Generate the standard deviations  $\sigma_{\tilde{S}_{mn}}$  and  $\sigma_{\tilde{S}_{m'n'}}$  as a function of the respective ranges  $d_{mn}$  and  $d_{m'n'}$  for nomadic links,

$$\log_{10}(\sigma_{\tilde{S}}) = \log_{10}(1.85) + 0.2 \log_{10} d + \sigma'_{\sigma_{\tilde{S}}}, \quad (5)$$

with  $\sigma'_{\sigma_{\tilde{S}}}$  being a zero-mean Gaussian distributed random variable standard deviation of 1.13, or equal to  $\sigma_{\bar{S}_o}$  for mobile links.

- Correlate both time series  $x(t)$  and  $y(t)$  at each time  $t$  using  $C[m, n, m', n']$ , to yield  $\tilde{S}_{mn}$  and  $\tilde{S}_{m'n'}$ .

#### C. Fading

The small-scale fading  $g_{mn}$  is best described in amplitude by a Ricean distribution in nomadic cases. The K-factor is related to the distance,

$$K|_{\text{dB}} = 16.90 - 5.25 \log_{10} \left( \frac{d}{d_0} \right) + \sigma'_K, \quad (6)$$

where  $\sigma'_K$  is a random Gaussian variable of deviation standard equal to 6 dB.

In mobile scenarios, the so-called second order scattering fading (SOSF) distribution is used to model the amplitude statistics [7],

$$p_{\text{SOSF}}(r) = r \int_0^\infty \omega e^{-w_1^2 \omega^2 / 4} \frac{4J_0(r\omega) J_0(w_0\omega)}{4 + w_2^2 \omega^2} d\omega, \quad (7)$$

where  $J_0$  is the Bessel function of the first kind and zero-th order. Note that  $E\{r^2\} = 1$  is achieved when  $w_0^2 + w_1^2 + w_2^2 = 1$  so that the distribution can be specified by two parameters,

$$\alpha = \frac{w_2^2}{w_0^2 + w_1^2 + w_2^2} \quad \text{and} \quad \beta = \frac{w_0^2}{w_0^2 + w_1^2 + w_2^2}, \quad (8)$$

where  $(\alpha, \beta)$  are constrained to the triangle  $\alpha \geq 0$ ,  $\beta \geq 0$ ,  $\alpha + \beta \leq 1$ . In each scenario,  $(\alpha, \beta)$  are randomly distributed as given by [7]

$$\begin{aligned} (\alpha, \beta) &\sim 0.09 \delta(\alpha) \cdot \mathcal{N}_{\mu=0.27, \sigma=0.14}(\beta) \\ &+ 0.59 \mathcal{N}_{\mu=0.40, \sigma=0.14}(\alpha) \cdot \delta(\beta) \\ &+ 0.32 \mathcal{N}_{\mu=[0.39, 0.24], \sigma=[0.12, 0.09], \rho=-0.13}(\alpha, \beta), \end{aligned} \quad (9)$$

for single-mobile links, and by

$$\begin{aligned} (\alpha, \beta) &\sim 0.03 \delta(\alpha) \cdot \mathcal{N}_{\mu=0.34, \sigma=0.16}(\beta) \\ &+ 0.72 \mathcal{N}_{\mu=0.54, \sigma=0.11}(\alpha) \cdot \delta(\beta) \\ &+ 0.25 \mathcal{N}_{\mu=[0.55, 0.19], \sigma=[0.14, 0.07], \rho=-0.52}(\alpha, \beta), \end{aligned} \quad (10)$$

for double-mobile scenarios. The fading processes between different links are modeled as independent variables.

TABLE I  
SHADOWING CORRELATION STATISTICAL MODEL

	Nomadic	Single-mobile		Double-mobile	
$(\mu_C, \sigma_C)$	(0,0.27)	common mov. (0.28,0.47)	no (mov.) common (0.00,0.36)	common mov. (0.29,0.39)	no (mov.) common (0.06,0.36)

#### IV. A CASE-STUDY APPLICATION OF THE MODEL: PARTNER SELECTION IN COOPERATIVE I2I NETWORKS

In the following example, the goal is to illustrate the importance of the channel model when assessing the trade-off between performance improvement and complexity increase for partner selection strategies based on the overall channel statistic instead of the average received power only.

##### A. System Model

The scenario under study consists of battery-powered nodes that are distributed indoors and communicate with a common access point (AP). The AP is acting as destination for all nodes. It propagates the synchronization signal to implement a time division multiple access (TDMA) scheme. The channel (path-loss, shadowing and fading) between the  $i$ -th node ( $i = 1, \dots, N$ ) and the  $j$ -th node ( $j = 0, \dots, N$ ), with node  $j = 0$  being the AP, is modeled as explained in the previous section, considering that indoor nodes are all static. In this preliminary analysis, the shadowing values are however assumed to be uncorrelated.

Cooperation is allowed by pairing the nodes analogous to [8], the node  $i$  in the pair  $(i, j)$  acting as an amplify-and-forward (AF) relay for the respective partner  $j$ . The AP communicates the cooperating partners, the time-slot assignments and the radio-frequency (RF) transmit powers. Depending on the AP decision, based on some knowledge of the multi-link channel statistic, a certain number of nodes are not required to act as relays.

##### B. Performance Analysis and Partner Selection Strategies

Assuming that the battery capacity is the same for all nodes, the network lifetime is by definition inversely proportional to the maximum energy expenditure among the nodes. The analysis of energy consumption within the network is carried out as detailed in [8] by targeting certain outage probability  $P_{\text{out}}$  and spectral efficiency  $R$  for all nodes. The network lifetime gain of AF cooperation, with respect to the direct transmission, is determined by the resource allocation strategy (pairing solution) implemented at the AP. The optimal pairing solution, that maximizes the network lifetime gain, is based on the whole knowledge of the multi-link channel statistic. Yet, (i) the uplink overhead increases since the AP must be updated with all the inter-node channel statistics; (ii) the combinatorial optimization algorithm that computes the optimal solution becomes too complex as the network size increases. To overcome these drawbacks, two low-complexity algorithms, the worst-link-first based on the uplink coding-gains (WLF-CG) and the same one based on the uplink path-loss values (WLF-PL), have been proposed and compared in [8]. For indoor-to-outdoor (I2O) communications, where the

uplink channel qualities dominate the outage performance, the WLF-CG algorithm maximizes the network lifetime. On the other hand, the WLF-PL obtains suboptimal performance with the advantage of being more robust to the inaccurate estimation of the distributed channel statistic.

In order to have the paper self-contained, we briefly overview the worst-link-first algorithm based on the metric  $m_{i,j}$  denoting a generic measure of the link  $(i, j)$  quality. In the first (distributed) phase, each node  $i$  estimates the ratio  $m_{i,j}/m_{i,0}$ , which represents how much better its link to the potential relay  $j$  is compared to a direct uplink connection without relay. If  $m_{i,j}/m_{i,0} > \eta$ , node  $j$  becomes a candidate partner for node  $i$ . At the end of this phase, each node communicates to the BS the set of candidate partners. In the final (centralized) phase, the BS builds a sorted list of nodes from the smallest (worst-uplink) to the largest uplink quality (best-uplink). At each iteration the BS assigns to the worst-uplink node its best-uplink candidate partner, if there is one, and removes the paired nodes from the list. If no candidate partners are available for the worst-uplink node, the BS leaves the node without partner and removes it from the list.

The quality of the links is measured by the inverse of the path loss  $m_{i,j} = L_{i,j}^{-1}$  for the WLF-PL algorithm and by the channel coding gain  $m_{i,j} = \frac{\exp K_{i,j}}{K_{i,j}+1} L_{i,j}^{-1}$  for the WLF-CG algorithm [8].

##### C. Simulation Results

Lifetime performances of the optimal and sub-optimal partner selection algorithms are here simulated for the I2I cooperative network presented in Section IV-A. Performance results are averaged over  $10^7$  scenarios. For each scenario,  $N$  nodes together with the AP are randomly distributed in a  $25\text{m} \times 25\text{m}$  indoor environment. The parameters  $(L_{i,j}, K_{i,j})$  values associated to every inter-node and uplink channel are stochastically generated as described in (2), with  $\sigma_{\bar{S}_o} = 4.4\text{dB}$ , and (6), respectively. The target outage probability is  $p = 10^{-3}$  for all the nodes with spectral efficiency  $R = 1$  bps/Hz. Gaussian modulation is assumed for both cooperative and direct transmissions.

Fig. 1 shows the ratio between the maximum energy consumptions, averaged among the scenarios, for the non-cooperative and cooperative systems, i.e. the network lifetime gain as defined in [8]. In Fig. 1-a, the performance of the low-complexity algorithms WLF-CG and WLF-PL are compared for different choices of the threshold  $\eta$  from 0 to  $10^2$ . Interestingly, the most conservative choice of  $\eta$  with respect to the inter-node channel quality ( $\eta = 10^2 < m_{i,j}/m_{i,0}$ ) provides the best performance of the WLF-CG algorithm, while it has a negative impact on the performance of the WLF-PL. In the latter case, many good pairing solutions are too early

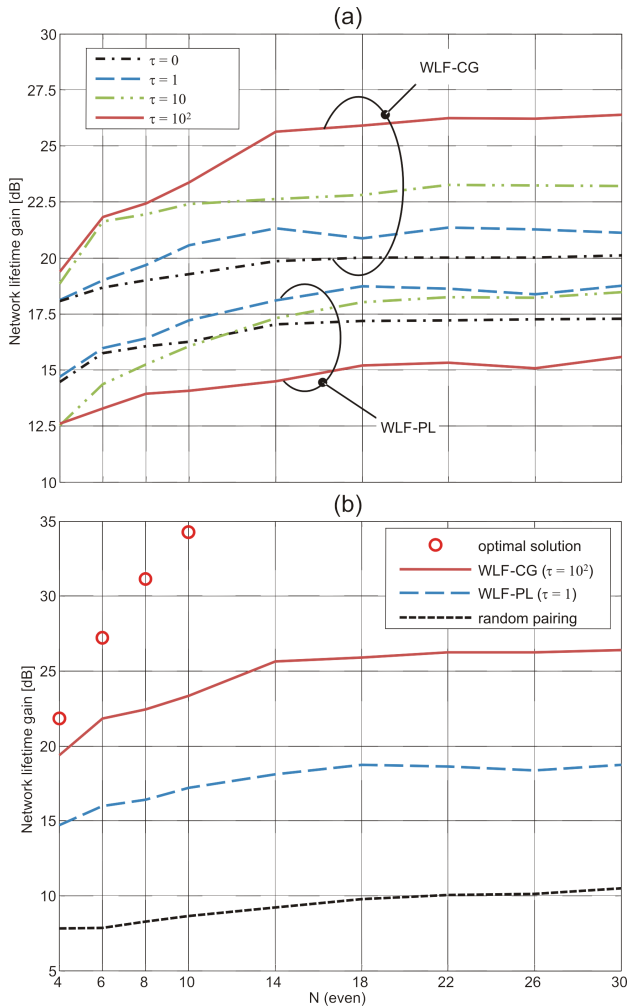


Fig. 1. Network lifetime gain of AF cooperation, compared to the non-cooperative transmission, vs. the number of nodes  $N$ : (a) The suboptimal WLF-CG and WLF-PL performance are evaluated for different threshold values  $\eta$ . (b) Optimal and suboptimal pairing strategies are compared.

excluded in the distributed phase of the WLF-PL algorithm. The best threshold choice for the WLF-PL algorithm is instead  $\eta = 1$ : the partner selection is the outcome of a well-balanced decision between the two phases of the algorithm, that allows the maximum exploitation of the incomplete knowledge of the channel statistics (i.e., the K-factors are unknown).

In Fig. 1-b, the optimal pairing solution (circle markers) is compared to the suboptimal algorithms WLF-CG (solid line) and WLF-PL (dashed line), implemented with the respective best choice of  $\eta$ . The random pairing strategy (dotted line) is also evaluated as in [8]. The degree of optimality of the WLF-CG is remarkably lower in the present I2I scenario compared to the I2O case of [8]. The latter result suggests that the complete knowledge of the inter-node channels statistics is crucial for the computation of the optimal pairing solution. Indeed, uplinks and the inter-user links qualities impact similarly the AF outage performances, as they have on average the same statistics. Although suboptimal for the considered I2I scenario, the partner selection strategies WLF-CG and WLF-PL increase the network lifetime by factors up to 400 and 50, respectively, compared to the non-cooperative transmission; by factors up to

40 and 5, respectively, compared to a random partner selection.

## V. CONCLUSIONS

This paper has proposed the implementation of an empirical model for indoor peer-to-peer cooperative channels, which takes into account path-loss, shadowing and fading in a comprehensive way. It namely includes a model of dynamic shadowing correlation, and rely, as much as possible, and in agreement with experimental data, on Gaussian-related distributions (e.g. Rayleigh, Rice, lognormal, SOSF, etc.). This implementation has then been applied to a case-study consisting in the evaluation of a cooperative network life for various channel-assisted partner selection strategies.

## VI. ACKNOWLEDGMENTS

This work was partially supported by the European Commission in the framework of the FP7 Network of Excellence in Wireless COMMUNICATIONS NEWCOM++ (contract no. 216715), by US Army grant W911NF-07-2-0027-1, by the Vienna Science and Technology Fund in the FTW project PUCCO, and by the European COST 2100 Action. The FTW Forschungszentrum Telekommunikation Wien is supported by the Austrian Government and the City of Vienna within the competence center program COMET. The work of C. Oestges is supported by the Belgian Fonds de la Recherche Scientifique (FRS-FNRS). The work of N. Czink is supported by an Erwin Schrodinger Fellowship of the Austrian Science Fund (FWF grant number J2789-N14). The work of B. Bandemer is supported by an Eric and Ileana Benhamou Stanford Graduate Fellowship. The work of P. Castiglione is supported by the Austria Science Fund (FWF) through grant NFN SISE (S106). The work of F. Kaltenberger is supported by the European Commission in the framework of the FP7 project SENDORA (contract no. 216076) and by Eurecom.

## REFERENCES

- [1] A. Sendonaris, E. Erkip, and B. Aazhang, "User cooperation diversity – part I: System description," *IEEE Trans. Commun.*, vol. 51, no. 11, pp. 1927–1938, Nov. 2003.
- [2] —, "User cooperation diversity – part II: Implementation aspects and performance analysis," *IEEE Trans. Commun.*, vol. 51, no. 11, pp. 1939–1948, Nov. 2003.
- [3] E. Beres and R. Adve, "Selection cooperation in multi-source cooperative networks," *IEEE Trans. Wireless Commun.*, vol. 7, no. 118–127, pp. 3013–3025, Jan. 2008.
- [4] P. Agrawal and N. Patwari, "Correlated link shadow fading in multi-hop wireless networks," *IEEE Trans. Wireless Commun.*, vol. 8, no. 8, pp. 4024–4036, Aug. 2009.
- [5] R. Madan, N. Metha, A. Molisch, and J. Zhang, "Energy-efficient cooperative relaying over fading channels with simple relay selection," *IEEE Trans. Wireless Commun.*, vol. 7, no. 8, pp. 3013–3025, Aug. 2008.
- [6] C. Oestges, N. Czink, B. Bandemer, P. Castiglione, F. Kaltenberger, and A. Paulraj, "Experimental characterization of indoor multi-link channels," in *Proc. IEEE Intl. Symposium on Personal, Indoor and Mobile Radio Communications (PIMRC)*, Tokyo, Japan, Sep. 2009.
- [7] B. Bandemer, C. Oestges, N. Czink, and A. Paulraj, "Physically motivated fast-fading model for indoor peer-to-peer channels," *Electronics Letters*, vol. 45, no. 10, pp. 515–517, May 2009.
- [8] P. Castiglione, S. Savazzi, M. Nicoli, and T. Zemen, "Impact of fading statistics on partner selection in indoor-to-outdoor cooperative networks," in *Proc. ICC 2010 - IEEE Int. Conf. Commun.*, Cape Town, South Africa, May 2010.